Effects of Re, Ta, and W in [110] (001) dislocation core of γ/γ' interface to Ni-based superalloys: First-principles study*

Chuanxi Zhu(朱传喜) and Tao Yu(于涛)†

Central Iron and Steel Research Institute, Beijing 100081, *China*

(Received 21 June 2020; revised manuscript received 3 August 2020; accepted manuscript online 7 August 2020)

The strengthening effects of alloying elements Re, Ta, and W in the [110] (001) dislocation core of the γ/γ' interface are studied by first-principles calculations. From the level of energy the substitution formation energies and the migration energies of alloying elements are computed and from the level of electron the differential charge density (DCD) and the partial density of states (PDOSs) are computed. Alloying elements above are found to tend to substitute for Al sites γ' phase by analyzing the substitution formation energy. The calculation results for the migration energies of alloying elements indicate that the stability of the [110] (001) dislocation core is enhanced by adding Ta, W, and Re and the strengthening effect of Re is the strongest. Our results agree with the relevant experiments. The electronic structure analysis indicates that the electronic interaction between Re-nearest neighbor (NN) Ni is the strongest. The reason why the doped atoms have different strengthening effects in the [110] (001) dislocation core is explained at the level of electron.

Keywords: Ni-based superalloys, dislocation structure, electronic structure, first-principles calculations

PACS: 61.82.Bg, 31.15.A−, 61.72.Lk, 31.15.ae **DOI:** 10.1088/1674-1056/abad26

1. Introduction

Ni-based superalloys, which have excellent high-temperature comprehensive properties, have been designed for use as industrial gas turbine blades and aerospace turbine blades. The microstructure of the superalloys consists of a high volume fraction of γ' ($L1_2$ structure)-precipitates, which are coherently embedded in the nickel solid solution γ (FCC structure)-matrix.[1,2] The difference between the lattice parameters of γ'-matrix and γ-matrix leads to the lattice misfit and related stress field in γ/γ' interface.[3] During high-temperature creep the dislocation network is formed in the γ/γ' interface for the purpose of relieving the misfit stress, which has an important effect on the creep strength of superalloys.[4–8] When the lattice misfit of γ-matrix and γ'-matrix is $-0.3\% \sim 0.3\%$, the dislocations of (001) interface in the network are screw with Burgers vectors of $1/2a\langle 110\rangle$. It has been reported that the interfacial dislocation network can improve the high-temperature creep resistance of superalloys, which is normally deposited in the (001) interface.[9–11] Alloying elements Ta, W, and Re can improve the creep rupture strength of superalloys,[12] and experiment has reported that the order of improvement in creep-strengthening is Ta < W < Re.[13] Alloying elements Ta, W, Re, Cr, Mo, Hf in the Ni/Ni_3Al interface of the Ni-based superalloys are found by atom probe tomography technology (APT).[14–17] Therefore, studying the interaction between alloying elements and dislocation core is very important for us to explore the influence of the alloying elements on the creep strength of superalloys.

The interfacial bonding strength determines the mechanical property of the superalloys.[18] Zhu *et al.*[19] found that there are only two atomic configurations in the Ni/Ni_3Al interface through the molecular dynamics (MD) simulation, one is the coherent region, and the other is the misfit dislocation region. It concluded that whether Re atom is added to the coherent region or the dislocation region the Re atom has a strong interaction with its NN Ni atoms. In our previous publication,[20] the influences of alloying elements on the mechanical properties of the γ/γ' interface which is in the coherent region were studied, and the effects of alloying elements on the mechanical properties of the γ/γ' interface is as follows: Ta < W < Re. Wang *et al.*[21] studied the site preferences of Ru and Re in the [110] (001) dislocation core and pointed out that Ru and Re tend to occupy the γ-Ni site. Geng *et al.*[22] studied the strengthening effects of W and Ta in [110] (001) dislocation core of the γ/γ' interface and found that the W and Ta significantly stabilize the [110] (001) dislocation core. Through adopting the first-principles method and the lattice Green-function multiscale method, Liu *et al.*[23] obtained the equilibrium geometry of the dislocation in the γ matrix and analyzed the electronic structure change caused by the addition of Re, Ta, and W. The diffusion behaviors of alloying elements influence the microstructure of crystal, which has a significant influence on the creep strength of superalloys. The diffusion rate of Re in Ni-based superalloys is low and the solute-vacancy exchange energy of Re is high, which confirms the strengthening effect of Re in superalloys.[24,25] Therefore, the migration energies of alloying elements can

*Project supported by the National Key Research and Development Program of China (Grant No. 2017YFB0701503).
†Corresponding author. E-mail: ytao012345@163.com
© 2020 Chinese Physical Society and IOP Publishing Ltd

be introduced to describe the interactions between X-NN Ni (X = Re, Ta, and W) in the dislocation core. Experiment has reported that the order of improvement in creep-strengthening is Ta < W < Re.[13] The strengthening effects of Ta, W, and Re on Ni-based superalloys were mainly focused on γ matrix, γ'-matrix, and the coherent region of the γ/γ' interface in previous studies,[19–27] so we will study the strengthening effects of the doped atoms in the dislocation core of the γ/γ' interface and explain the reason why the doped atoms have different strengthening effects in the [110] (001) dislocation core at electronic level.

In this paper, the first-principles calculation method executed by Vienna *ab initio* simulation package (VASP)[28,29] is picked to study the site preferences and strengthening effects of Re, Ta, and W in the [110] (001) dislocation core. The details of computational model and method are given in Section 2. In Subsection 3.1, the substitution formation energies are calculated so as to explore the site preferences of the doped atoms in the dislocation core. In Subsection 3.2, the migration energies of alloying elements are calculated in order to describe the interaction between X-NN Ni (X = Re, Ta, and W). It is known that only one electron dissimilarity exists among Re, W, and Ta atoms, however their effects on creep properties of Ni-based superalloys are different. In order to explore this problem, the DCD and PDOSs are analyzed and discussed in Subsections 3.3 and 3.4, respectively. The key research outcomes are summarized in Section 4.

2. Computational model and methods

The model of [110] (001) dislocation is constructed as follows. The model includes the γ-Ni, γ'-Ni_3Al, and γ/γ' interface, and the lattice parameters of γ'-Ni_3Al and γ-Ni are 3.567 Å and 3.52 Å,[30] respectively. The model is composed of $37.5 \times 37.5 \times 15$ γ-Ni unit cells and $37 \times 37 \times 15$ γ'-Ni_3Al unit cells in the [110], [−110], [001] directions. The model contains 333030 atoms. The box vectors are selected in order to ensure the Burgers vector of the dislocation is $(1/2)\langle 110\rangle$ type, which is consistent with the experiment.[31] In the X and Y directions the model takes periodic boundary condition, and in the Z direction the model takes free surface boundary condition. The dislocation of γ/γ' interface is formed by MD simulation using the embedded-atom method potential of Ni–Al[30] and the atomic arrangement of misfit dislocation is presented in Fig. 1. There are two equivalent dislocation core structures in the Ni/Ni_3Al interface, one is the [110] (001) dislocation and the other is the [−110] (001) dislocation, therefore the [110] (001) dislocation is chosen to research the strengthening effects of alloying elements in [110] (001) dislocation core.

We choose 200 atoms around the [110] (001) dislocation core as our calculation model. The size of model is large enough to understand the interactions between alloying elements and [110] (001) dislocation. The model of the [110] (001) dislocation core is displayed in Fig. 2. A vacuum layer is added in the X and Z directions respectively, and the thickness of the vacuum layer is 12 Å. The model contains eight atomic layers with *ABCDABCD* stacking sequence along [−110] direction, which is displayed in Fig. 3. The three different alloying elements X = Re, Ta, and W are considered in this paper. Eight substituting positions in the dislocation core are selected, as displayed in Fig. 3. When relaxing the [110] (001) dislocation core models, the outermost atoms of the model are fixed to keep the overall dislocation structure unchanged.

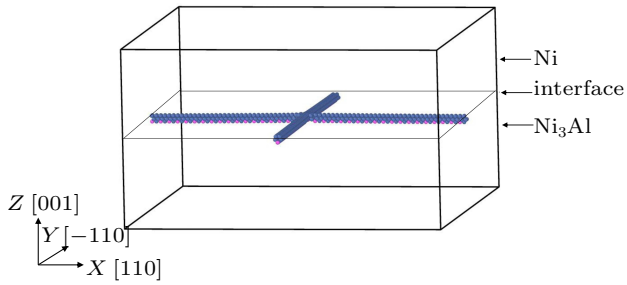

Fig. 1. The [110] (001) dislocation of the γ/γ' interface. The red balls and blue balls denote Al atoms and Ni atoms, respectively.

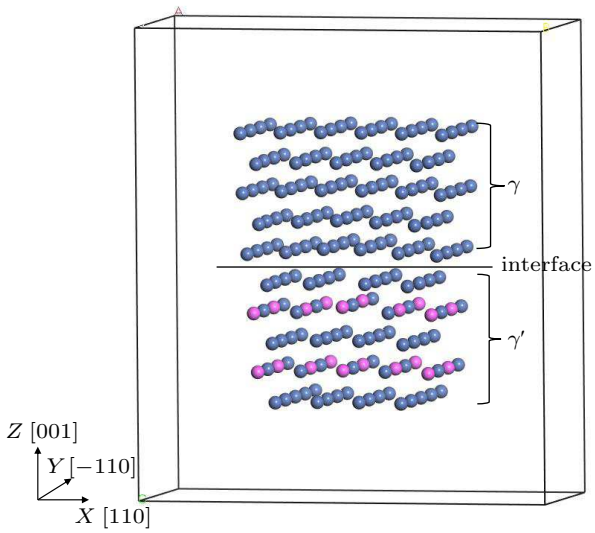

Fig. 2. The model of the [110] (001) dislocation core in γ/γ' interface. The color atoms in the figure correspond to Al and Ni atoms in Fig. 1, respectively.

The total-energy calculations are implemented by the plane wave-based VASP[28,29] through applying the projector augmented wave (PAW) method[32,33] in the present study. The Perdew–Burke–Ernzerhof (PBE)[34] exchange–correlation functional within the generalized gradient approximation (GGA) is applied. The Monkhorst–Pack k-point mesh is set to be $1 \times 4 \times 1$ for the model of [110] (001) dislocation core. The energy cutoff of plane-wave basis set is 400 eV. All atomic positions are completely relaxed until the Hellman–Feynman forces acting on the atoms are below 0.02 eV/Å. The

migration energies of alloying elements in the [110] (001) dislocation core are calculated by the method of climbing image nudged elastic band.[35] Three images are selected from the initial configuration to the final configuration and the maximum forces on the atoms are smaller than 0.02 eV/Å.

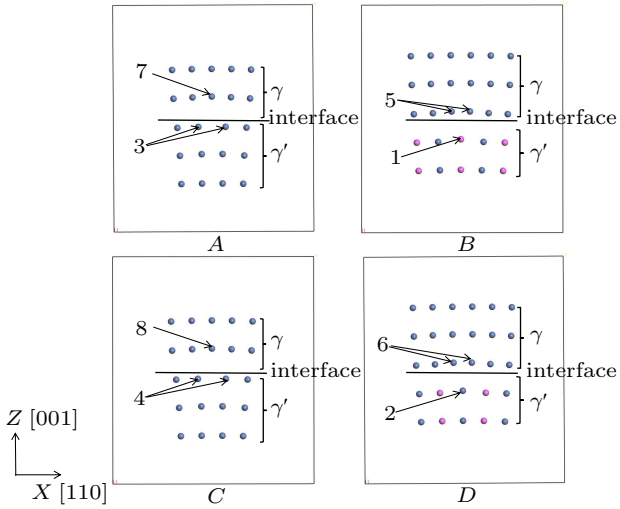

Fig. 3. The planes A, B, C, and D stack along $[-110]$ direction. Eight substitution sites are: $1^{\gamma'\text{-Al}}$, $2^{\gamma'\text{-Ni}^1}$, $3^{\gamma'\text{-Ni}^2}$, $4^{\gamma'\text{-Ni}^3}$, 5^{γ-Ni^1}, 6^{γ-Ni^2}, 7^{γ-Ni^3}, and 8^{γ-Ni^4}. The color atoms in the figure correspond to Al and Ni atoms in Fig. 1, respectively.

3. Results and discussion

3.1. Site preferences of alloying elements in the [110] (001) dislocation core

In previous study[20] the site preferences of Re, Ta, and W in the coherent region of γ/γ' interface were investigated by calculating the substitution formation energies. The site preferences of Re, Ta, and W in the dislocation region of γ/γ' interface is under discussion. Before studying the strengthening effects of the doped atoms, the site preferences of Re, Ta, and W in the dislocation core should be investigated. Figure 3 shows that the alloying elements substitute for $1^{\gamma'\text{-Al}}$, $2^{\gamma'\text{-Ni}^1}$, $3^{\gamma'\text{-Ni}^2}$, $4^{\gamma'\text{-Ni}^3}$, 5^{γ-Ni^1}, 6^{γ-Ni^2}, 7^{γ-Ni^3}, and 8^{γ-Ni^4}, respectively. The substitution formation energies of the doped atoms are derived as follows:[20,36,37]

$$E^{X\text{ in }\gamma'}_{\text{sub, Ni or Al}} = \frac{1}{n}\left[\left(E^{X\text{ in }\gamma'} + n\mu_{\text{Ni/Al}}\right) - \left(E^{\gamma'} + n\mu_X\right)\right], \quad (1)$$

$$E^{X\text{ in }\gamma}_{\text{sub, Ni}} = \frac{1}{n}\left[\left(E^{X\text{ in }\gamma} + n\mu_{\text{Ni}}\right) - \left(E^{\gamma} + n\mu_X\right)\right], \quad (2)$$

where X represents Re, Ta, and W, $E^{X\text{ in }\gamma'}$ represents the total energy of the X-doped system for substituting γ'-Ni and γ'-Al, and $E^{X\text{ in }\gamma}$ represents the total energy of the X-doped system for substituting γ-Ni. Parameter n represents the number of the doped atom. According to the definition of chemical potential, the chemical potential of an atom is equal to the energy of a single atom in the elementary substance. $\mu_{\text{Ni/Al}}$ represents the chemical potential of Ni or Al, and μ_{Ni} is the total energy per atom in fcc-Ni unit cell. $\mu_{\text{Ni}_3\text{Al}}$ is equal to $3\mu_{\text{Ni}} + \mu_{\text{Al}}$, therefore μ_{Al} is equal to $\mu_{\text{Ni}_3\text{Al}} - 3\mu_{\text{Ni}}$. μ_X represents the chemical potential of alloying element. μ_{Re}, μ_{Ta}, and μ_{W} are the energies per atom in hcp-Re, bcc-Ta, and bcc-W unit cells, respectively. The computed results are listed in Table 1.

Table 1. The substitution formation energies (in unit eV) of the doped atoms which substitute for $1^{\gamma'\text{-Al}}$, $2^{\gamma'\text{-Ni}^1}$, $3^{\gamma'\text{-Ni}^2}$, $4^{\gamma'\text{-Ni}^3}$, 5^{γ-Ni^1}, 6^{γ-Ni^2}, 7^{γ-Ni^3}, and 8^{γ-Ni^4}, respectively.

Substituting site	The doped atoms		
	Re	Ta	W
$1^{\gamma'\text{-Al}}$	−0.45	−2.10	−0.97
$2^{\gamma'\text{-Ni}^1}$	0.36	−0.87	0.15
$3^{\gamma'\text{-Ni}^2}$	0.42	−0.87	0.12
$4^{\gamma'\text{-Ni}^3}$	0.34	−0.90	0.04
5^{γ-Ni^1}	0.17	−0.55	0.11
6^{γ-Ni^2}	0.15	−0.62	0.09
7^{γ-Ni^3}	−0.26	−1.15	−0.50
8^{γ-Ni^4}	−0.29	−1.22	−0.55

According to Table 1, for the Re substitution case the substitution formation energies of Re at $1^{\gamma'-Al}$, 7^{γ-Ni^3}, and 8^{γ-Ni^4} sites are negative and at $2^{\gamma'\text{-Ni}^1}$, $3^{\gamma'\text{-Ni}^2}$, $4^{\gamma'\text{-Ni}^3}$, 5^{γ-Ni^1}, and 6^{γ-Ni^2} sites are positive. The substitution formation energy of Re at $1^{\gamma'}$-Al site is the smallest, which means that Re prefers to occupy the γ'-Al site in the dislocation core. Also it has been found that Ta and W atoms also prefer to occupy the γ'-Al site in the dislocation core. This is in keeping with the APT experiment.[20]

3.2. The migration energies of alloying elements

It has been found that the doped atoms are prone to occupy the Al sites in the dislocation core by analyzing the substitution formation energies, therefore only the migration energies of the doped atoms occupying the Al site are calculated. Before calculating the migration energies of the doped atoms, the vacancy formation energies of the NN Ni atoms around the doped atom should be discussed. Which direction is easier to diffuse for the doped atom in the dislocation core can be found by analyzing the vacancy formation energies of the Ni atoms. The vacancy formation energies of the inequivalent Ni atoms around the doped atoms and the Al atom are calculated. Figure 4 displays the atomic distribution around the doped atom. The vacancy formation energy for Ni atom is derived as follows:[38,39]

$$E^{\text{f}}_{\text{Va}} = E_{\text{Va}} - E + E_{\text{atom}}, \quad (3)$$

where E_{Va} is the energy of the model with vacancy, E is the energy of the model without vacancy, and E_{atom} is the total energy per atom in fcc-Ni unit cell. The computed vacancy formation energies are presented in Table 2.

As can be seen from Table 2, the vacancy formation energy of Ni136 atom is the smallest, which means that the Ni136 atom site is most likely to form the vacancy around the doped atoms and the Al atom. When studying the diffusion behavior of the doped atom, the diffusion path from the doped

atom site to the Ni136 atom site is selected. When the doped atom is jump from one lattice site to another neighboring site, a driving energy is needed to defeat the lattice barriers and at which point the doped atom accomplishes a jumping motion. The energy needed is called as the migration energy and is defined as follows:[35]

$$E^{\mathrm{m}} = E_{\mathrm{sad}} - E_{\mathrm{min}}, \tag{4}$$

where E_{min} and E_{sad} denote the energies of initial and saddle point states respectively. The computed migration energies are presented in Table 3.

Table 2. The vacancy formation energies (in unit eV) for the inequivalent Ni atoms around the doped atoms and the Al atom.

Inequivalent Ni atom	Doped atoms and Al atom			
	Al	Re	Ta	W
Ni136	1.35	1.58	1.46	1.56
Ni43	1.58	1.62	1.69	1.67
Ni141	1.64	1.79	1.69	1.81
Ni138	1.67	1.79	1.76	1.80

Table 3. The migration energies (in unit eV) of the doped atoms and the Al atom in the dislocation core.

Migration energy	Doped atoms and Al atom			
	Al	Re	Ta	W
E^{m}	0.56	1.20	0.89	1.11

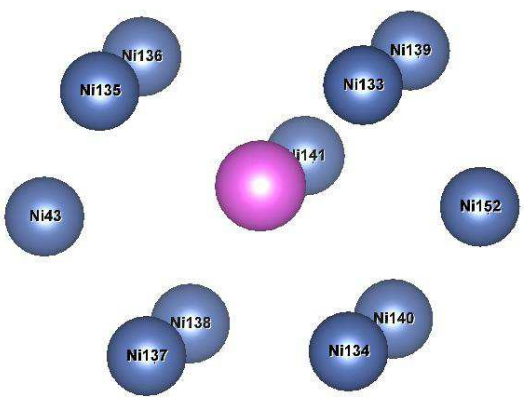

Fig. 4. The atomic distribution around the doped atom. The green ball denotes the doped atom and the blue balls denote Ni atoms. Ni152, Ni141, Ni140, Ni139, Ni138, Ni137, Ni136, Ni135, Ni134, Ni133, and Ni43 are the NN Ni atoms of the doped atom.

From Table 3, it should be noted that the migration energies of the doped atoms are larger than the migration energy of the Al atom, which means that the interaction between Al-NN Ni is weaker than that between X-NN Ni (X = Re, Ta, and W). The larger the migration energy is, the stronger the interaction between X-NN Ni (X = Re, Ta, and W) is. The migration energy calculations show that Ta, W, and Re can stabilize the dislocation core, and the order of stabilizing the dislocation core is shown as follows: Re > W > Ta. The stability of interfacial dislocation is vital for the creep performance of Ni-based superalloys. Experiment has reported that the order of improvement in creep-strengthening is Re > W > Ta.[13] and our calculation results are consistent with the experiment. In order to explore the reasons for the doped atoms having different strengthening effects in dislocation core, the effects of alloying elements on the local structure of the dislocation core are discussed. The average distance between X-NN Ni (X = Re, Ta, and W) is computed, and the results are presented in Table 4.

Table 4. The average distance (in unit Å) between X-NN Ni (X = Re, Ta, and W).

Re	Ta	W
2.600	2.644	2.613

From Table 4, the order of the average distance X-NN Ni (X = Re, Ta, and W) is Re < W < Ta, which means that it is more difficult for Re atom to overcome lattice barriers when the doped atoms diffuse in the dislocation core. So, the migration energy of Ta is the smallest and the migration energy of Re is the largest. In order to further explore the reasons for the doped atoms having different strengthening effects in the dislocation core, the bonding strength between X-NN Ni (X = Re, Ta, and W) should be studied, and the electronic structures are analyzed in Subsection 3.3.

3.3. Electronic structure analysis

3.3.1. The DCD analysis

The DCD[20,22] of the dislocation core doped with Re, Ta, and W is shown in Fig. 5. It has been found that the alloying elements prefer to substitute for Al sites in the dislocation core, so the charge accumulations between X-NN Ni (X = Re, Ta, and W) are discussed only when the doped atoms substitute for γ'-Al sites. As can be seen from Fig. 5, the charge density is increased between X-NN Ni (X = Re, Ta, and W), which means that there exists the charge accumulation between X-NN Ni (X = Re, Ta, and W). This shows that there is strong electronic interaction between X-NN Ni (X = Re, Ta, and W) and the bonding for the X-NN Ni (X = Re, Ta, and W) is stronger than that for the Al-NN Ni. Therefore, the Re, W, and Ta can stabilize the dislocation core. Further observation of the charge accumulation in the dislocation core region shows that there are strong charge accumulation regions appearing between the doped atoms and Ni140, Ni139, Ni138, Ni137, Ni136 Ni135, Ni134, and Ni133 atoms (Ni139, Ni136, Ni135, and Ni133 are equivalent; Ni140, Ni138, Ni137, and Ni134 are equivalent), which indicates that the aggregation of charges is directional. Thus, relatively strong bonds are formed between the doped atoms and Ni140, Ni139, Ni138, Ni137, Ni136 Ni135, Ni134, and Ni133 atoms and the bonding strength is increased too, which is beneficial for stabilizing the dislocation core.

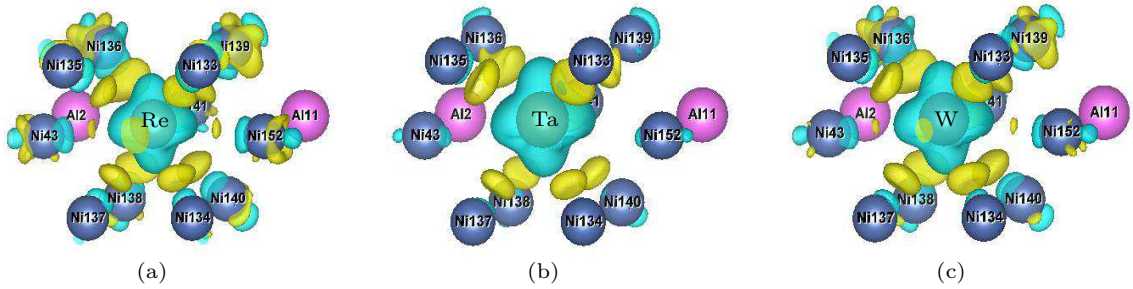

Fig. 5. The DCD of the dislocation core doped with Re, Ta, and W. Panel (a) is for the case where Re substitutes for the γ'-Al site; panel (b) is for the case where Ta substitutes for the γ'-Al site; panel (c) is for the case where W substitutes for the γ'-Al site. The blue and yellow regions denote charge loss and accumulation, respectively. The isosurface is 0.0045 e/Å^3. Ni152, Ni141, Ni140, Ni139, Ni138, Ni137, Ni136, Ni135, Ni134, Ni133, and Ni43 are the NN Ni atoms of the doped atom.

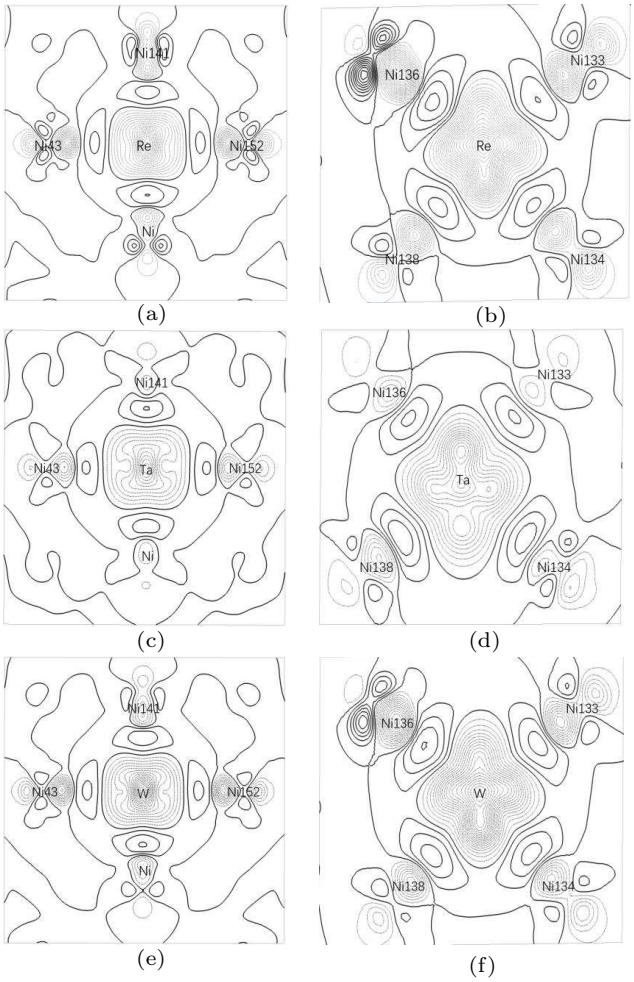

Fig. 6. Charge density contour plots of the dislocation core on the (001) plane and (120) plane. Panels (a), (c), and (e) are the charge density contour plots of the (001) plane that the Re, Ta, and W substitute for γ'-Al site, respectively; panels (b), (d) and (f) are the charge density contour plots of the (120) plane that the Re, Ta, and W substitute for γ'-Al site, respectively. Dashed and solid lines denote the decreased and the increased charge density, respectively. The contour spacing is 0.002 e/a.u.^{3}.

In order to explained the reason why the doped atoms have different strengthening effects in the [110] (001) dislocation core at electronic level, charge density contour plots of the dislocation core are shown in Fig. 6. From the point of charge transfer[20] when the doped atoms and their NN Ni atoms lose charges, the charges are transferred to the region between X-NN Ni (X = Re, Ta, and W). Re atom and its NN Ni atoms lose the most charges, and Ta atom and its NN Ni atoms lose the least charges. Therefore, the order of charge aggregation between X-NN Ni (X = Re, Ta, and W) is: Re > W > Ta, which means that the order of electronic interaction between X-NN Ni (X = Re, Ta, and W) is Re > W > Ta. Thus, the migration energy of the Re atom is the largest and the migration energy of the Ta atom is the smallest when the doped atoms diffuse in the dislocation core.

3.3.2. The PDOSs analysis

In order to analyze the hybridization between X-NN Ni (X = Re, Ta, and W), the PDOSs of the doped atoms and their NN Ni atoms are calculated. PDOSs of Re, Ta, W, and their NN Ni atoms in the dislocation core are shown in Fig. 7. The NN inequivalent Ni atoms of the doped atoms are Ni43, Ni136, Ni138, and Ni14. From Figs. 5 and 6, it can be found that there is a little charge accumulation between X-Ni43 (X = Re, Ta, and W), which indicates that the electronic interaction between X-Ni43 (X = Re, Ta, and W) is weak, so only the PDOSs of the doped atoms, Ni136, Ni138, and Ni141 are analyzed. In Fig. 7, it can be found that the s-orbital PDOSs and the p-orbital PDOSs of the NN inequivalent Ni atoms for the doped atoms are almost unchanged after the doped atoms substituted for the γ'-Al sites, and the d-orbital PDOSs of Ni atoms are moved toward to the lower energy level. The main peaks of the d-orbital PDOSs for the doped atoms and Ni atoms are located at the same low energy levels, so there exists strong d–d hybridization between X-NN Ni (X = Re, Ta, and W). It indicates that the electronic interaction between X-NN Ni (X = Re, Ta, and W) is stronger than that between the Al-NN Ni and it contributes to the d–d hybridization, therefore only the d–d hybridization between the X-NN Ni (X = Re, Ta, and W) are considered. The strengths of d-orbital PDOSs for Ni atoms are decreased at the Fermi level after the doped atoms substituted for the γ'-Al sites, which indicates that the transition probability of the electronic states is confined and the stability of the dislocation core can be increased.[19,20] A deep valley well separates the bonding and antibonding parts of X–d (X = Re, Ta, and

W) orbital PDOS near the Fermi level, which can increase the stability of the dislocation core.[40,41]

In Fig. 7, it can be seen that the hybridization between Re–Ni136 is mainly from Re–d orbital and Ni136–d orbital, because the d orbital PDOS of Re and the d-orbital PDOS of Ni136 have a peak at the same low energy level, so there is a strong d–d hybridization between Re and Ni136. The d–d hybridization state between Re–Ni136 occurs at −4.35 eV, and the strength of the corresponding hybridization peak for Ni136 is 0.39 eV^{-1}. The d–d hybridization state between Ta–Ni136 occurs at −4.14 eV and the strength of the corresponding hybridization peak for Ni136 is 0.29 eV^{-1}. There exists the d–d hybridization between W–Ni136 when the W substitutes for the γ'-Al site, and the strength of the corresponding hybridization peak for Ni136 is 0.31 eV^{-1} at −4.27 eV. The d–d hybridization between Re–Ni136 is stronger than that between W–Ni136 due to the hybridization peak moving to the lower energy level and the increased strength of hybridization peak.[20,23] Similarly, it can also be found that the d–d hybridization between W–Ni136 is stronger than that between Ta–Ni136.

There exists the d–d hybridization state between Re–Ni138 when the Re substitutes for the γ'-Al site, the d–d hybridization state between Re–Ni138 occurs at −4.35 eV, and the strength of the corresponding hybridization peak for Ni138 is 0.33 eV^{-1}. There exists the d–d hybridization between W–Ni138 and the strength of the corresponding hybridization peak for Ni138 is 0.31 eV^{-1} at −4.27 eV. There is no d–d hybridization state between Ta–Ni138 in the deep energy level, and it means the d–d hybridization between Ta–Ni138 is the weakest. The d–d hybridization between Re–Ni138 is stronger than that between W–Ni138.

Similarly, the d–d hybridization state between Re–Ni141 is analyzed, the d–d hybridization state between Re–Ni141 occurs at −4.35 eV, and the strength of the corresponding hybridization peak for Ni141 is 0.42 eV^{-1}. The d–d hybridization state between Ta–Ni141 occurs at −4.14 eV and the strength of the corresponding hybridization peak for Ni141 is 0.24 eV^{-1}. There exists the d–d hybridization between W–Ni141 when the W substitutes for the γ'-Al site, and the strength of the corresponding hybridization peak for Ni141 is 0.34 eV^{-1} at −4.27 eV. Therefore, the d–d hybridization between Re–Ni141 is stronger than that between W–Ni141, and the d–d hybridization between W–Ni141 is stronger than that between Ta–Ni141.

From above analyses, it can be concluded that the d–d hybridization between Ta–NN Ni is the weakest and the d–d hybridization between Re–NN Ni is the strongest. Therefore, the migration energy of the Re atom is the largest and the migration energy of the Ta atom is the smallest when the doped atoms diffuse in the dislocation core, and the order of stabilizing the dislocation core is shown as follows: Re > W > Ta.

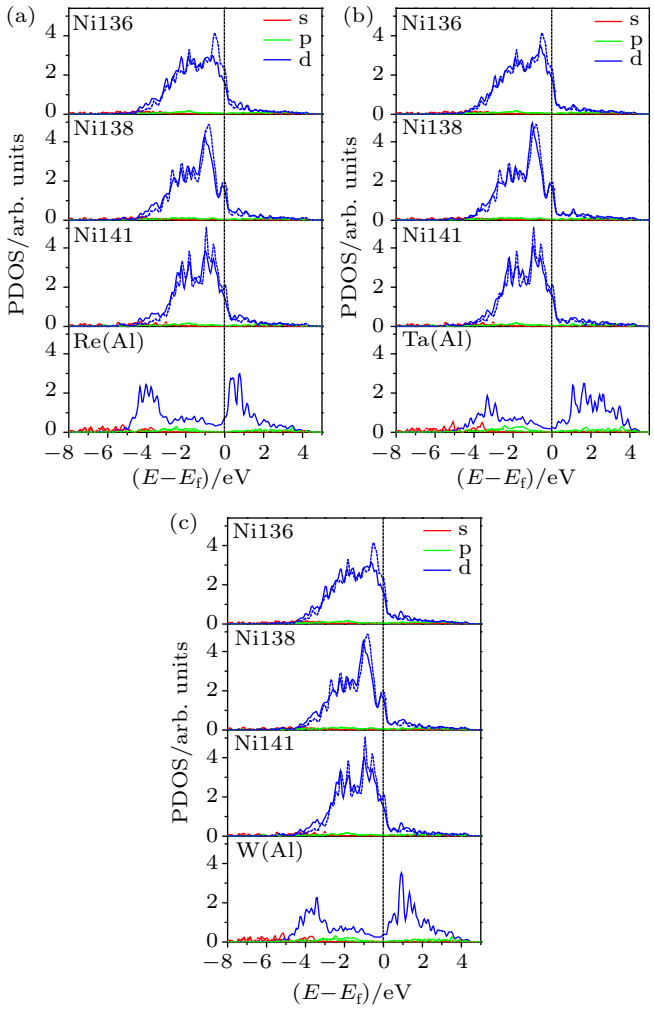

Fig. 7. The PDOSs of the doped atoms and their NN Ni atoms in the dislocation core. The Fermi energies are shifted to zero. The dashed lines and solid lines represent the PDOSs without and with (a) Re, (b) Ta, and (c) W, respectively.

4. Conclusion

In this paper, the strengthening effects of Re, Ta, and W atoms in the [110] (001) dislocation core of the Ni/Ni_3Al interface have been studied by first-principles calculations. We found that the doped atoms tend to substitute for the γ'-Al site in the [110] (001) dislocation core. The migration energies of the doped atoms are calculated, the results indicate that Re, W and Ta can stabilize the [110] (001) dislocation core, and Re exhibits the best strengthening effect. We also found that the Re needs to overcome the most lattice barriers compared to Ta and W when the doped atoms diffuse in the dislocation core. The order of stabilizing the dislocation core is shown as follows: Re > W > Ta. The electronic structure analysis indicates that there are strong electronic interactions between X-NN Ni (X = Re, Ta, and W). The d–d hybridization between Ta–NN Ni is the weakest and the d–d hybridization between Re–NN Ni is the strongest. The reason why the doped atoms have different strengthening effects in the [110] (001) disloca-

tion core is explained at electronic level.

References

[1] Reed R C 2006 *The Superalloys: Fundamentals and Applications* (Cambridge University Press) p. 102
[2] Durand-Charre M 1997 *The Microstructure of Superalloys* (CRC Press)
[3] Pollock T M and Argon A S 1992 *Acta Metal. Mater.* **40** 1
[4] Jacome L A, Nörtershäuser P, Somsen C, Dlouhý A and Eggeler G 2014 *Acta Mater.* **69** 246
[5] Link T, Epishin A, Bruckner U and Portella P 2000 *Acta Mater.* **48** 1981
[6] Yue Q Z, Liu L, Yang W C, Huang T W, Zhang J and Fu H Z 2019 *Mater. Sci. Eng. A* **742** 132
[7] Zhang J X, Wang J C, Harada H and Koizumi Y 2005 *Acta Mater.* **53** 4623
[8] Ding Q Q, Li S Z, Chen L Q, Han X D, Zhang Z, Yu Q and Li J X 2018 *Acta Mater.* **154** 137
[9] Hantcherli M, Pettinari-Sturmel F, Viguier B, Douin J and Coujou A 2012 *Scr. Mater.* **66** 143
[10] Luo Z P, Wu Z T and Miller D J 2003 *Mater. Sci. Eng. A* **354** 358
[11] Tian S G, Zhou H H, Zhang J H, Yang H C, Xu Y B and Hu Z Q 2000 *Mater. Sci. Eng. A* **279** 160
[12] Erickson G L 1995 *JOM.* **47** 36
[13] Reed R C 2006 *The Superalloys: Fundamentals and Applications* (Cambridge University Press) pp. 157–158
[14] Bagot P A J, Silk O B W, Douglas J O, Pedrazzini S, Crudden D J, Martin T L, Hardy M C, Moody M P and Reed R C 2017 *Acta Mater.* **125** 156
[15] Tu Y Y, Mao Z G and Seidman D N 2012 *Appl. Phys. Lett.* **101** 121910
[16] Amouyal Y, Mao Z G and Seidman D N 2010 *Acta Mater.* **58** 5898
[17] Wu X X, Makineni S K, Liebscher C H, Dehm G, Rezaei Mianroodi J, Shanthraj P, Svendsen B, Burger D, Eggeler G, Raabe D and Gault B 2020 *Nat. Commun.* **11** 389
[18] Reed R C 2006 *The Superalloys: Fundamentals and Applications* (Cambridge University Press) p. 46
[19] Zhu T, Wang C Y and Gan Y 2010 *Acta Mater.* **58** 2045
[20] Zhu C X, Yu T, Wang C Y and Wang D W 2020 *Comput. Mater. Sci.* **175** 109586
[21] Wang C and Wang C Y 2009 *Chin. Phys. B* **18** 3928
[22] Geng C Y, Wang C Y and Yu T 2005 *Physica B* **358** 314
[23] Liu F H and Wang C Y 2017 *RSC Adv.* **7** 19124
[24] Janotti A, Krčmar M, Fu C L and Reed R C 2004 *Phys. Rev. Lett.* **92** 085901
[25] Zhang X M, Deng H Q, Xiao S F, Zhang Z, Tang J F, Deng L and Hu W Y 2014 *J. Alloys Compd.* **588** 163
[26] Yu X X and Wang C Y 2012 *Mater. Sci. Eng. A* **539** 38
[27] Wen M R and Wang C Y 2017 *Chin. Phys. B* **26** 093106
[28] Kresse G and Hafner J 1993 *Phys. Rev. B* **47** 558
[29] Kresse G and Furthmüller J 1996 *Phys. Rev. B* **54** 11169
[30] Du J P, Wang C Y and Yu T 2013 *Modell. Simul. Mater. Sci. Eng.* **21** 015007
[31] Buffiere J Y and Ignat M 1995 *Acta Metall. Mater.* **43** 1791
[32] Blöchl P E 1994 *Phys. Rev. B* **50** 17953
[33] Kresse G and Joubert D 1999 *Phys. Rev. B* **59** 1758
[34] Perdew J P, Burke K and Ernzerhof M 1996 *Phys. Rev. Lett.* **77** 3865
[35] Henkelman G, Uberuaga B P and Jónsson H 2000 *J. Chem. Phys.* **113** 9901
[36] Liu S H, Liu C P, Liu W Q, Zhang X N, Yan P and Wang C Y 2016 *Philos. Mag.* **96** 2204
[37] Kohan A F, Ceder G, Morgan D and Van de Walle C G 2000 *Phys. Rev. B* **61** 15019
[38] Liu S H, Wen M R, Li Z, Liu W Q, Yan P and Wang C Y 2017 *Mater. Des.* **130** 157
[39] Liu S H, Li Z and Wang C Y 2017 *Chin. Phys. B* **26** 093102
[40] Wen M R and Wang C Y 2016 *RSC Adv.* **6** 77489
[41] Wang D W, Wang C Y, Yu T and Liu W Q 2020 *Chin. Phys. B* **29** 043103